Chapter 8
Magnetically Enhanced Centrifugation for Industrial Use

Johannes Lindner, Karsten Keller, Gunnar Grim, Johannes Feller, Christian Fiil Nielsen, Niels Dalgaard, Katharina Menzel and Hermann Nirschl

Abstract Magnetically enhanced centrifugation is a new approach in high-gradient magnetic separation possible in continuous mode, which promises a large potential for industrial use. Magnetic particles are separated to a wire filter, from which they are cleaned by centrifugal forces to the chamber wall. The simulation of magnetic particles collected by a wire were possible by the discrete element method. The simulation shows the detachment of particles from the wires by the centrifugal force. Two prototype machines were set up to investigate the process. The discharge of particles from the wire filter depends on the magnetic field strength and the centrifugal velocity. It was possible to set up a machine reaching a separation efficiency of 99 % at a volume flow of 1 m^3/h (excluding dead times) in a batch-wise mode. A second machine built as magnetically enhanced decanter separates particles and transports them out of the bowl by a screw conveyor in a completely continuous mode. Instead of the common electromagnets a permanent magnet assembly can be combined with a magnetically enhanced centrifuge to save costs.

J. Lindner (✉) · G. Grim · J. Feller · C.F. Nielsen · N. Dalgaard · K. Menzel
Mechanical Process Engineering and Mechanics, Karlsruhe Institute of Technology, Karlsruhe, Germany
e-mail: Johannes.lindner@kit.edu

K. Keller
DuPont, Wilmington, DE 19980, USA
e-mail: Karsten.Keller@dupont.com

H. Nirschl
Institute of Mechanical Process Engineering and Mechanics, Karlsruhe Institute of Technology, 76131 Karlsruhe, Germany
e-mail: hermann.nirschl@kit.edu

H. Nirschl and K. Keller (eds.), *Upscaling of Bio-Nano-Processes*,
Lecture Notes in Bioengineering, DOI 10.1007/978-3-662-43899-2_8

8.1 Introduction

High-gradient magnetic separation (HGMS) is a method for the separation of magnetic matter from liquid. It is based on a magnetic wire filter inserted in a chamber. The wires are magnetized by an external magnet (Svoboda 2004). A suspension passes through the chamber and the particles deposit on the wires by magnetic forces. The discharge is enabled by removing the magnet to release the particles from the wires. Then the chamber is flushed back to discharge the magnetic particles. Calculations for the filter capacity of a primitive cell are shown in (Ebner et al. 2007). A quasi-continuous HGMS variant is a carousel which enables a quick swapping of chambers for quasi-continuous use (Franzreb 2001). A different approach for magnetic separation is magnetic cake filtration (Eichholz et al. 2011; Eichholz et al. 2008).

A process based on magnetic functionalized particles would be an interesting alternative to adsorption chromatography or expanded bed adsorption. The kinetics of adsorption and elution are in this case fast, while the fluid flow in a batch-wise process is the limiting factor for the kinetics in the process. A particle-based process might allow lower cycle times and a continuous process, resulting in a more efficient use of the expensive functionalization. A Magnetically enhanced centrifuge (MEC) separates magnetic particles continuously. A star-shaped magnetic wire filter is integrated in the centrifuge. It is placed inside a magnet, which magnetizes the wire filter. Particles are separated to the wire filter and are discharged continuously to the wall in large agglomerates by centrifugal forces. The parameters that influence the MEC process are already published (Lindner et al. 2010; Lindner et al. 2013a). A continuous discharge of the particles from the decanter wall is possible, one possibility is by a decanter screw (Lindner and Nirschl 2014). This is necessary in order to take advantage of the low-adsorption cycle times of micron-scaled particles. Different approaches for the simulation of magnetic separation have already been executed (Hournkumnuard and Chantrapornchai 2011; Gerber and Birss 1983). The simulation is important for the optimization of separation. Additionally, influences such as magnetically induced agglomeration have an important influence on separation (Lindner et al. 2013b).

This chapter deals with the possibilities of MEC for industrial use. A simulation is shown combining finite element modeling (FEM) of the magnetic field around a wire with a discrete element model for magnetic particles. The core of the chapter is a batch-wise industry centrifuge set up by Andritz KMPT. It handles volume flow of up to 1 m^3/h at high separation efficiency. A longitudinal permanent magnet arrangement is introduced, which was optimized for and tested with MEC. A test on a decanter centrifuge is shown to demonstrate its capabilities as a continuous device.

8.2 Theory

The equations shown below were used to simulate a particle collection on a wire. The force on a magnetic particle depends on the field gradient. Distortion of an external field allows high gradients. The magnetic force of the gradient of a field

H on a particle of magnetization M_P and volume V_P is, with the magnetic permeability μ_0 (Svoboda 2004):

$$\partial F_m = \mu_0 M_P \nabla H \partial V_P \tag{8.1}$$

Satoh used the magnetic dipole force for the simulation of magnetic particles (Satoh et al. 1998). The dipole–dipole force between two particles can be simplified for particles aligned in the direction of a homogenous magnetic field. A discussion on assumptions made in this approach can be found in (Lindner et al. 2013b). The following equation was used in a discrete element model simulation:

$$F_{m,ij} = -\frac{3\mu_0 m_{Pi} m_{Pj}}{4\pi} \frac{1}{r_{ij}^4} \begin{pmatrix} \left(5 * t_x^2 - 3\right) t_x \\ \left(5 * t_x^2 - 1\right) t_y \\ \left(5 * t_x^2 - 1\right) t_z \end{pmatrix} \tag{8.2}$$

The centrifugal force F_Z on a particle is given by the particle mass m, the rotational speed ω, and the radius r.

$$F_Z = -m * \omega \times (\omega \times r) \tag{8.3}$$

The mechanic force $F_{n,ij}$ used in the simulation was implemented based on a spring-damper model with the coefficients k_n and $\eta_{n,ij}$, the normal overlap δ in normal direction n_{ij} in the spring part, and the relative normal velocity $v_{rel,n,ij}$ in the damper model (Lindner et al. 2013b; Deen et al. 2007; Langston et al. 1995).

$$F_{n,ij} = k_n \delta^{3/2} n_{ij} - \eta_{n,ij} * v_{rel,n,ij} \tag{8.4}$$

$\boldsymbol{F}_{t,ij}$ is the tangential frictional force proportional to the tangential sliding velocity $\boldsymbol{v}_{rel,t,ij}$. It is necessary to reduce the sliding of particles since without this force, a particle tends to oscillate around the dipole end of another particle.

$$F_{t,ij} = -\eta_{t,ij} * v_{rel,n,ij} \tag{8.5}$$

The parameters are summarized in Table 8.1.

8.2.1 Considerations for Scaling

Separation efficiency of one wire for a certain volume flow of HGMS scales with fluid velocity $v_0^{-1/3}$ as long as $v_m / v_0 \gg 1$. The velocity of a particle in proximity to a

Table 8.1 Overview over simulation parameters

Parameter	Equation	Parameter	Equation
Normal stiffness	$k_{n,ij} = \frac{4}{3}\sqrt{r_{eq}} E_{eq}$	Normal damping	$\eta_{n,ij} = 0.3 * \sqrt{\frac{9}{2} m_{eq} \sqrt{\delta} k_{n,ij}}$
Tangential stiffness	$k_{t,ij} = \frac{2\sqrt{2R_{eq}} G_{eq}}{2-\upsilon} \sqrt{\delta}$	Tangential damping	$\eta_{t,ij} = 2\sqrt{\frac{2}{7} m_{eq} k_{t,ij}}$
Equalized mass	$m_{eq}^{-1} = m_i^{-1} + m_j^{-1}$	Equalized radius	$r_{eq}^{-1} = r_i^{-1} + r_j^{-1}$
Equalized rigidity modulus	$G_{eq}^{-1} = \frac{1-\upsilon_i^2}{G_i} + \frac{1-\upsilon_j^2}{G_j}$	Equalized elasticity modulus	$E_{eq}^{-1} = \frac{1-\upsilon_i^2}{E_i} + \frac{1-\upsilon_j^2}{E_j}$

wire v_m is deduced from the resistance force of fluid and the magnetic force (Watson 1973). Parameters are the particle diameter b, the wire diameter a, the fluid viscosity η, the wire magnetization M_D, and $\Delta\kappa$, the volume susceptibility difference between the fluid and the particle (Svoboda 2004; Gerber and Birss 1983).

$$v_m = \frac{2}{9}\mu_0 \Delta\kappa M_D H_0 \frac{b^2}{a\eta} \tag{8.6}$$

It is hence possible to scale the volume flow linear with the volume of the filter cell and magnet, enabling the setup of larger centrifuges than those presented in this work.

8.3 Simulation of Magnetically Enhanced Centrifugation

The discrete element method allows the simulation of particle deposition by calculating forces between particles. In case of HGMS, it is necessary to implement as well the magnetic forces between particles, which are essentially dipole forces.

8.3.1 Simulation Results

The commercial program EDEM 2.3 from DEM Solutions was used as software platform with a custom contact model implemented for the simulation of particle deposition in HGMS and MEC. Equation (8.2) was implemented as a custom contact force for magnetic interparticular forces. Equations (8.3) and (8.4) were implemented as mechanical models. To simulate the force resulting from the magnetic wire, a finite element simulation was done with the software Comsol 3.4. The field gradient around a cylinder was calculated and read in EDEM. Equation (8.1) was implemented to calculate the force of the wire on particles.

The magnetic field around a dipole is enhanced on two opposite sides parallel to the field direction. Perpendicular to the field direction, the background field is weakened. As magnetic matter is attracted by strong field regions and repulsed by weak regions, particles agglomerate in needle shape. An important assumption is that the mutual influence of each particle's magnetization may be neglected if both particles are in saturation magnetization. Distant magnetic forces were cut off after a specific distance to stabilize the simulation and to reduce computational effort. A time step of 10^{-5} s was applied in the simulation (Table 8.2).

The simulation was performed in order to better understand the behavior of particles in the magnetic field. A simulation was done with the magnetic field of a round wire read in the DEM model. For a certain time, particles collected on top of the wire. Figure 8.1 left shows the deposit of magnetic particles on a wire without centrifugal force. The centrifugal force was added as constant acceleration in Fig. 8.1 right. The particles leave the wire, with some notable deposits left at the end of the wire. A high gradient at the wire end showed to retain particles. The simulation showed needle-shaped agglomeration before the particles settle on the wire and after detaching.

Table 8.2 Parameters in the simulation

Symbol	Value	Unit	Denotation
M_P	480 000	[A/m]	Particle magnetization (except given otherwise)
ν	0.3	[-]	Poisson ratio
E	$2*10^5$	[Pa]	Elasticity modulus
ρ_P	2 000	[kg/m^3]	Density Particle
R	$0.5*10^{-6}$	[m]	Physical particle radius (mechanic force)
r_c	$4*10^{-6}$	[m]	Contact radius (magnetic force)
v	0.001	[m/s]	Initial velocity
a	$5*10^{-4}$	[m]	Wire radius
b	$1*10^{-5}$	[m]	Particle radius (except given otherwise)
M_W	$1.6*10^6$	[A/m]	Wire magnetization

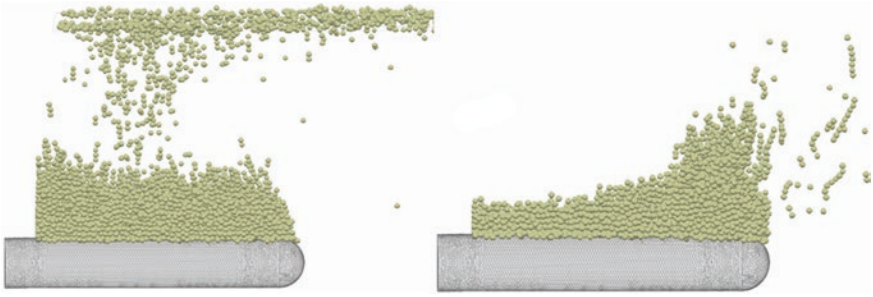

Fig. 8.1 Deposit of magnetic particles on a wire in a HGMS process without centrifugal force (*left*) and with centrifugal force (*right*)

8.3.2 Validation

Figure 8.2 shows a comparison of particle deposits seen in the HGMS experiment and particle deposition calculated in the simulation. In the validation experiment, footage of the particle deposit on a wire is shown. It was produced by inserting an endoscope into a HGMS cell. A cut wire was introduced within the cell to be able to observe particle separation from the side of the wire. Bayferrox magnetite was used as magnetic matter. An electromagnet was installed outside of the cell, with the magnetic field pointing in the same direction as the fluid flows. The deposit of particles on the wire points in the direction of the inlet, with few particles attaching to the side opposite of the inlet. Repulsive zones on the sides of the wire show no collection of particles. A film was produced during separation, from which the picture in Fig. 8.2 (left) was taken. It showed a defined particle deposit shape, which is characteristic for HGMS. The experiment showed the attachment of particles to the wire upstream of the flow. The deposit still increased past what is shown in Fig. 8.2 (left) and is barely limited.

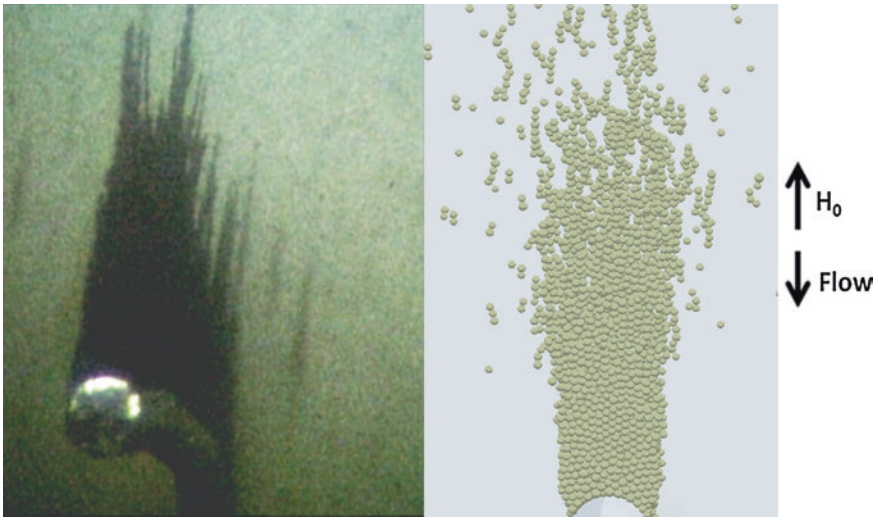

Fig. 8.2 Comparison of magnetic deposit in an HGMS process (*left*) with simulated deposit (*right*)

Figure 8.2 (right) shows a simulation of 100 µm particles collected on a 1 mm wire. The deposit shows a dense structure close to the wire which gets porous at a distance from the wire. The simulation fits the experiment well, despite the difference in particle size. Needle-shaped agglomeration is observable in the fluid. The same shape is visible as well in the simulation.

In summary, simulation and experiment agree well. The discrete element method delivers good results for the comparison of the simulation of magnetic suspensions.

8.4 Batch-Wise Magnetically Enhanced Centrifugation in Industrial Scale

For the investigation of magnetic separation, an industrial-scale machine was set up. It is batch-wise to limit the amount of particles and fluid, but shows separation comparable to the continuous version shown in Sect. 8.5.

8.4.1 Setup

The industrial-scale machine, shown in Fig. 8.3, was set up to show that the volume flow in the range of 1 m^3/h is realistic. It was manufactured by Andritz KMPT.

Fig. 8.3 The industrial-scale MEC (*left*) with the blue electromagnet installed around the machine; the machine is fed from the bottom and discharges at the top; a window is installed in the top to allow study of particle deposits; the wire matrix after cleaning (*right*)

The centrifuge is sealed, and a Plexiglas cover allows the fluid outlet to be viewed to supervise cleanliness and wire coverage. Tests were performed in a pilot line set up at a Solae plant in Aarhus, Denmark. The centrifuge chamber in the magnet has a volume of 6 l. The MEC was fed out of a container by a piston pump, which delivered up to 1 m^3/h. The diameter is 250 mm and the maximum rotational velocity is 4 000 rpm. Blades for preacceleration at the inlet and to avoid swirling at the outlet were implemented. The magnet installed around the machine delivers a flux density of up to 0.4 T at the center of the device. The matrix installed turns at a differential velocity of 120 rpm to disperse the particles. The concentration was measured gravimetrically by weighing the container, the suspension, and the particle mass after drying. Samples were washed to eliminate contamination. Merck MagPrep Silica particles, which are commercially available, were used for the separation tests. The density is 3.25 g/cm^3 and the saturation magnetization is 67 Am^2/kg.

8.4.2 Wire Cleaning by Centrifugal Forces

Figure 8.4 left shows wires covered with magnetic particles after stopping the centrifuge from 2 250 rpm at a flux density of 240 mT. Centrifugation allows the particle deposit to be cleaned from the wires to the wall. A sufficiently high rotational speed allowed the wires to be completely cleaned. Figure 8.4 right shows a photograph taken after centrifuging at 240 mT and 3 000 rpm. A clear line in the center of the wire is visible.

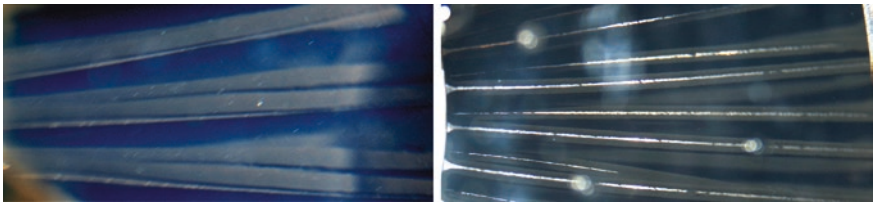

Fig. 8.4 Wires were covered with magnetic particles by magnetism, then the centrifugal force was increased to discrete velocities to test wire discharge; at 240 mT and centrifugation at 2 250 rpm wires are still completely covered (*top*); at 240 mT and 3 000 rpm a *center line* is clean while particles are still attached to wire edges (*bottom*)

Fig. 8.5 Cleaning of filter wires by centrifugal forces depends on the magnetic field; the relation seems to be quadratic

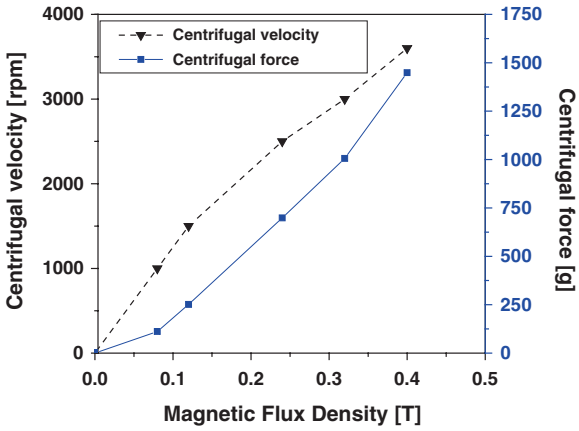

The cleaning of the wire in Fig. 8.4 was used as a criterion to determine the correlation for the wire cleaning between the centrifugal velocity and the magnetic field. The rotational speed necessary was determined at different magnetic field strengths to discharge particles from the center line. The results are shown in Fig. 8.5. The relation seems to be linear for centrifugal velocity, and calculated to be quadratic for centrifugal force. Saturation magnetization of particles and wires did not show to reduce the necessary centrifugal force. A consequence is the necessity of increasing the centrifugal velocity if the magnetic flux density is increased.

8.4.3 Performance

The industrial-scale centrifuge was set up to demonstrate the potential of the process for handling large particle amounts. The separation efficiency was determined by the concentration of feed and effluent.

$$\eta = 1 - \frac{c_{Feed}}{c_{Effluent}} \tag{8.7}$$

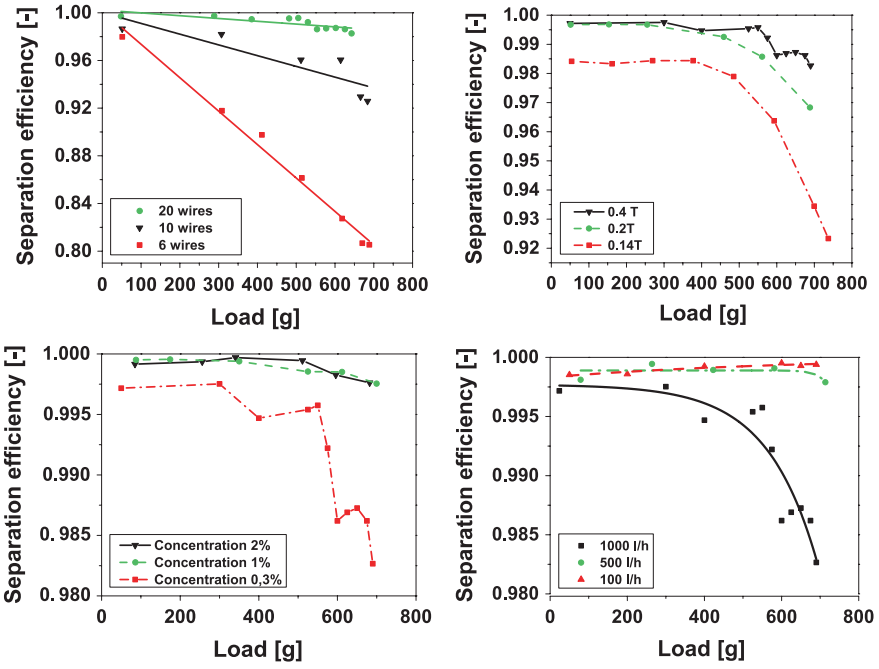

Fig. 8.6 Load over time depends on the number of wire stages implemented in the device (*top left*, 500 l/h; 1 000 rpm; 0.3 wt%; 0.4 T), on the flux density (*top right*, 1 000 l/h; 1 000 rpm; 0.3 wt%; 20 wire stages in matrix) and on the particle concentration (*bottom left*, 1 000 l/h; 1 000 rpm; 0.4 T; 20 wire stages); a completely filled device with 20 matrix wire stages allows high particle load, while separation is slightly reduced at 10 wires and heavily reduced at 6 wire stages; Separation over load at different volume flow (*bottom right*, 1 000 rpm; 0.4 T; 0.3 wt%; 20 wire stages): high volume flow reduces the amount of separated particles, especially at high loads

The centrifuge stored more than 600 g of particles and handled volume flows of up to 1 000 l/h (excluding dead times for the discharge). Figure 8.6 shows the influence of different parameters on the separation during the filling of the centrifuge. Figure 8.6 top left documents the behavior of particle deposits in the machine over time for a different number of wire stages. With 20 wire stages built into the machine, the separation was more than 99.7 % and close to the analytic measuring limit. At high load, the efficiency dropped after loading 500 g of particles. Introducing lower wire numbers led to a slightly lower separation value of 98.7 % at 10 wires at low load. Taking into account that the measurement was taken at a volume flow of 1 000 l/h, the separation was still at a high level. With 6 wire stages in the machine and a filling of more than 600 g, separation dropped significantly to 81 %.

Figure 8.6 top right shows the influence of the flux density over varying particle loads. There was no significant difference in the experiment between 0.4 and 0.2 T up to the limit of the device capacity. A drop of the flux density to 0.14 T

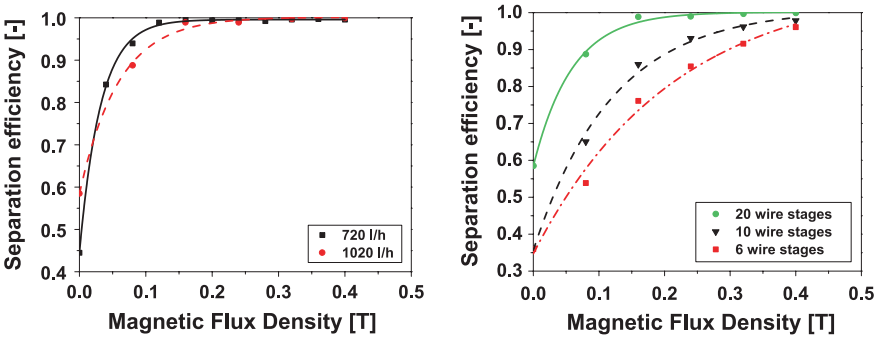

Fig. 8.7 The separation over the magnetic field for a different number of wire stages (*left*, 1 000 rpm; 0.3 w%; 20 wire stages) and for different volume flow (*right*, 1 000 l/h; 1 000 rpm; 0.3 w%) shows a significant influence; a volume flow of 1 m^3/h allows high separation efficiency; at low magnetic field strengths, low volume flow increases separation efficiency

reduces separation from 99.7 to 98.4 %. The reason for this is the saturation of the magnetization of the wires and particles at about 0.2 T. Figure 8.6 bottom left shows the influence of the concentration at different loads. A logarithmic influence was documented in Lindner et al. (2013a). In this experiment with particle load, no significant drop was noticed from 2 to 1 %, but a slight drop when the concentration was reduced to 0.3 % magnetic matter. The concentration influences the separation because of its effect on the agglomeration of particles. In Fig. 8.6 bottom right, the influence of different volume flows for different loads is shown. At 1 000 l/h, separation drops below 99 % at 600 g load. At a lower volume flow of 500 or 100 l/h, separation is almost unchanged when the centrifuge is filled with up to 700 g. The magnetic flux density is the most important influence for separation.

The influence of the flux density at varying volume flow and wire stages was investigated as well. Figure 8.7 left shows the separation behavior at high volume flow for different magnetic field strengths. Separation was good at 99 % from 0.2 T on, even for 1 m^3/h. At low magnetic flux density, a volume flow of 720 l/h proved to reduce separation to a lesser extent. Without a magnetic field applied, the separation showed unsteady results around 50 % separation which are caused by turbulence introduced at the inlet of the centrifuge. A different number of wire stages in Fig. 8.7 right showed a much higher influence at 1 000 l/h than in the previous experiment at 500 l/h in Fig. 8.6 top left.

8.4.4 Discharge in a Batch-Wise Magnetically Enhanced Centrifuge

Redispersion of the batch-wise machine was done by flushing 10 l of liquid in a cycle for 5 min while stirring the matrix at 120 rpm, and for another 5 min without

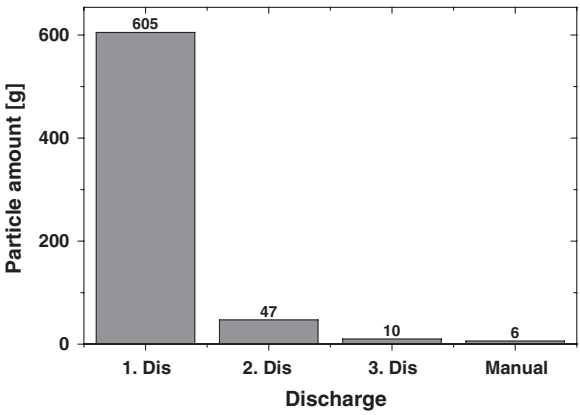

Fig. 8.8 Discharge characteristics: particle amounts discharged by redispersing in three batches in 10 l liquid each; redispersing was done by pumping in a cycle during 5 and 5 min matrix stirring; manual discharge by removing filter matrix and flushing manually 1.5 Continuous Magnetically Enhanced Centrifugation

stirring. Then the machine was drained and the suspension collected. The machine was filled again with washing water. The redispersion method was repeated before displacing the washing water and repeating the discharge a third time. The concentration and volume were measured each time. Then the matrix was unloaded, chamber and matrix were flushed manually, and the particle amount was again determined. Figure 8.8 shows the result of the discharge experiment. While a batch-wise centrifuge did not take advantage of the potential of the process in continuous mode, it is possible to use this device in a batch-wise automatic process.

8.5 Continuous Magnetically Enhanced Centrifugation

Besides the batch-wise magnetically enhanced centrifuge, a continuous centrifuge design was set up and tested. It performed similar to the batch-wise centrifuges in terms of separation, but it is used continuously.

8.5.1 Setup

Figure 8.9 left shows a decanter screw with a wire matrix implemented in the cylindrical part (Lindner and Nirschl 2014). Figure 8.9 right shows the complete decanter centrifuge set up at the Karlsruhe Institute of Technology. The screw is integrated into the centrifuge. Within the decanter screw, a magnetizable wire filter is installed in the cylindrical inner part. An electromagnet is installed around the centrifuge. The centrifuge is sealed to control the pressure. This is necessary in order to achieve different fill levels, like in a siphon, in the cylindrical part and conic part of the centrifuge. The cylindrical part is filled with liquid, covering the wire filter completely. The conic part is filled with particles at a lower fill level. Particles flow through a tube in the screw and are fed in between the cylindrical and conic parts. In the cylindrical part, particles are collected on

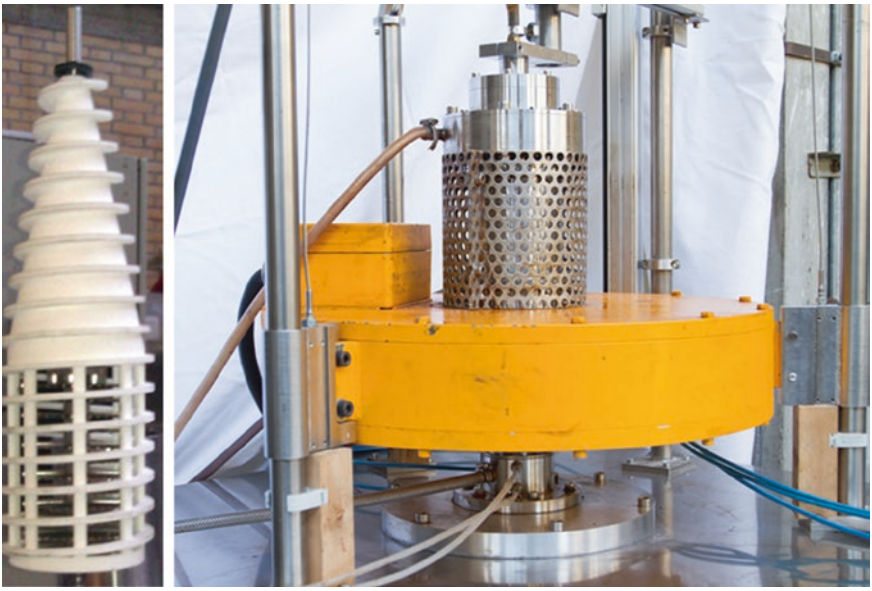

Fig. 8.9 The decanter screw is mounted on the shaft (*left*) with the bowl next to it, inside of the screw a wire filter is implemented; Magnetic decanter assembled with yellow magnet (*right*), feed inlet on top; the particle discharge is next to it linked with a hose for the flushing of particles; the particle discharge is at the bottom. Additionally, hoses are connected to cool the seals

the wall and separated from the liquid by the screw, which transports them over the cone and out of the liquid. They are collected in a round container on top of the device. Clean water flushes particles out, flowing from a tangential inlet, swirling through the container, and is discharged tangentially through a second hose. The particles, having dried and shed the original liquid in the decanter cone, are now in clean liquid. In our tests the cleaned particle-free effluent was used to flush the particles from the container back into the stirred feed tank to realize a continuous process at steady state in a cycle. The electromagnet created a flux density of 0.2 T. A volume flow of 50 l/h was used. In the system, 200 g of particles in 8 l of demineralized water circulated in the cycle. The decanter did not transport particle amounts below 100 g. The particles used in this test are still in development and are less efficient in separation compared to the Merck MagPrep Silica used in the Andritz KMPT centrifuge. The particle kind used is research-grade and has a saturation magnetization of 47 Am^2/kg and a remanence of 11 Am^2/kg.

8.5.2 Continuous Separation

The separation showed to be mainly dependent on the magnetic field, while the centrifugal force was necessary to convey particles out of the machine. Figure 8.10 shows the concentration of fluid discharge and particle discharge. The separation

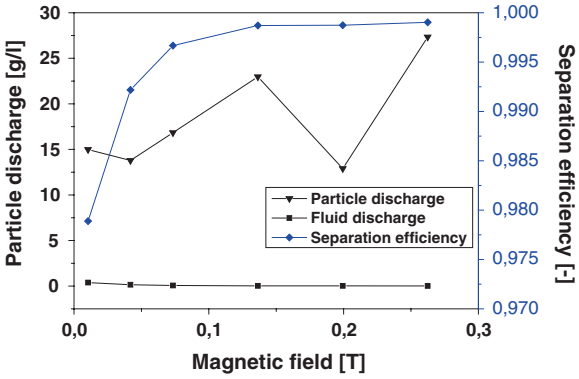

Fig. 8.10 Influence of magnetic field strength in a magnetically enhanced decanter (1 650 rpm; 54 l/h; 2 wt%; 11 wire stages)

efficiency is shown as second axis, rising from 62 % without magnetic flux to 99 % at 0.33 T. The whole separation process was tested successfully at steady state for several hours at a volume flow of 50 l/h.

The continuous magnetically enhanced centrifuge proves to be capable of continuously separating magnetic particles at high volume flow. Two requirements for the use in a continuous pilot line for protein separation are:

- a centrifuge for each process step is required in a continuous process, resulting in at least two for separation after adsorption and elution;
- the high cleaning effort and particle loss when stopping the machine, together with the high minimum fluid and particle amount (200 g) make the machine inappropriate for tests of low volume.

It is an interesting option for industrial production at large scale though, while batch-wise HGMS devices are more interesting for the processing of low particle amounts.

8.6 Permanent Magnet Arrangement for Magnetically Enhanced Centrifugation

HGMS bases either on conventional permanent magnets or on electromagnets. While conventional permanent magnets do not create a field in a longitudinal direction necessary for MEC, electromagnets are expensive in investment and operation. An alternative is the use of a permanent magnet arrangement creating a field in axial direction.

8.6.1 Setup

The design was deduced from the work of Hugon (Hugon et al. 2010a, b) on a patent of Aubert. Hugon investigated an arrangement, which allowed the generation

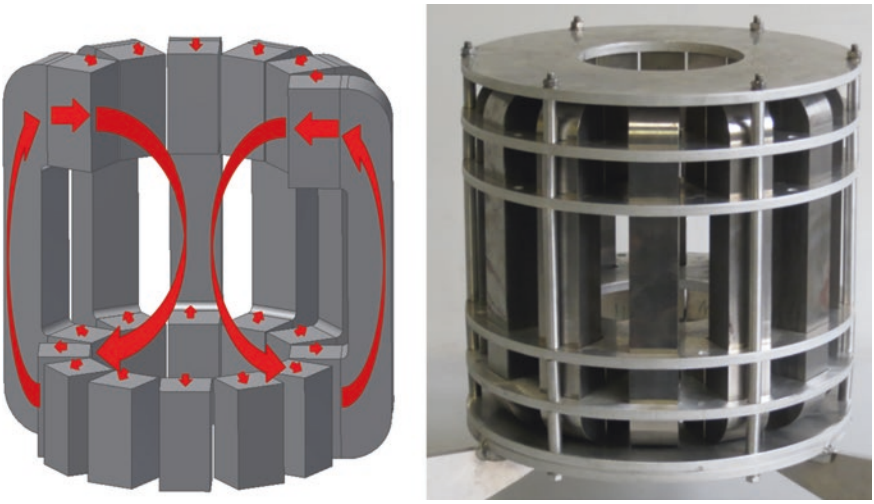

Fig. 8.11 Principle and setup magnet of the longitudinal magnet arrangement

of a field rotationally symmetric to an axis and longitudinal in axis direction. Magnets are arranged in two circles. In the top magnet circle, the magnet north pole points inwards, whereas in the bottom magnet circle north pole points outwards. The arrangement is large compared to the original magnet set up by Hugon at an inner magnet diameter of 125 and 120 mm of spacing between the top and bottom circles. The magnet was improved by finite element modeling set up at the Karlsruhe Institute of Technology. An improvement resulting from FEM was the implementation of pole yokes to close the field lines on the outside and enhance the field in the center. Additionally, the magnet was enhanced by implementing magnets which are longish ($35 \times 35 \times 70$ mm^3). The magnetic flux density was hence increased to 230 mT, but has a significant gradient at the magnet surface. The principle is shown in Fig. 8.11 left and the magnet in Fig. 8.11 right.

8.6.2 Performance of the Permanent Magnet Arrangement Compared to an Electromagnet

The longitudinal permanent magnet arrangement was tested on a batch-wise pilot MEC. The centrifuge was already presented with an electromagnet in (Lindner et al. 2013). While the flux density is weaker than that of a classic permanent magnet of comparable size of 0.4 T and a Halbach magnet of 0.32 T, those magnets' fields cannot be aligned with the centrifuge axis. An electromagnet has a less homogeneous field but can be more easily controlled by adjusting the current. In industrial machines, the use of electromagnets is limited by their high electricity consumption and the fact that they are prone to overheating.

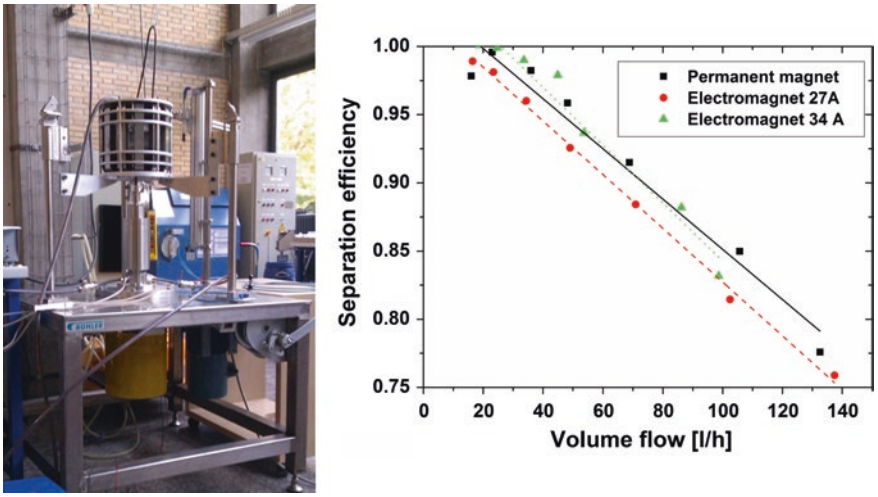

Fig. 8.12 The permanent magnet mounted on the batch-wise centrifuge; Influence of the volume flow on separation with electromagnet at 0.23 T in the center (*34 A*) and at the wall (*27 A*): permanent magnet separation is in between the two values

In the tests, a rotational velocity of 1 500 rpm was used, corresponding to 63 times the acceleration of the earth's gravity. Figure 8.12 left shows the magnet mounted on top of the centrifuge. It was installed with a cable pull, to allow it to be removed upwards from the MEC. This removes the magnetic field, which is necessary for the discharge of the device. During the separation test, it was placed around the centrifuge center. The separation of the magnet was tested at different volume flows in Fig. 8.12 right. A comparison with an electromagnet at the same magnetic flux density of 0.23 T in the center (34 A) and at the wall (27 A) was done. The separation efficiency was shown to be at a level similar to the comparison experiment.

8.7 Conclusion

A simulation of one MEC wire was performed, revealing agglomeration before separation and long particle chains when particles detach from the wire. The validation of the simulation was possible. MEC is a promising technology for the separation of magnetic particles. The amount of particle deposit on a wire is a function of the centrifugal velocity and the magnetic field. Separation of up to 1 m^3/h in a pilot machine was possible. A continuous process proved to be possible using a decanter approach. This is an interesting option for the processing of large volumes in pilot lines. A permanent magnet was developed which showed similar separation compared to an electromagnet. It reduces investment cost, machine weight, and energy cost drastically.

References

Deen NG et al (2007) Review of discrete particle modeling of fluidized beds. Chem Eng Sci 62(1–2):28–44

Ebner NA et al (2007) Filter capacity predictions for the capture of magnetic Microparticles by high-gradient magnetic separation. IEEE Trans Magn 43(5):1941–1949

Eichholz C et al (2011) Recovery of lysozyme from hen egg white by selective magnetic cake filtration. Eng Life Sci 11(1):75–83

Eichholz C et al (2008) Magnetic field enhanced cake filtration of superparamagnetic PVAc-particles. Chem Eng Sci 63(12):3193–3200

Franzreb M (2001) New design of high-gradient magnetic separators using permanent magnets. In: Proceedings of 6th world congress of chemical engineering, Melbourne, Australia, 23–27 Sept 2001

Gerber R, Birss RR (1983) High gradient magnetic separation. Research Studies Press, New York

Hournkumnuard K, Chantrapornchai C (2011) Parallel simulation of concentration dynamics of nano-particles in high gradient magnetic separation. Simul Model Pract Theory 19(2):847–871

Hugon C et al (2010a) Design, fabrication and evaluation of a low-cost homogeneous portable permanent magnet for NMR and MRI. Comptes Rendus Chimie 13(4):388–393

Hugon C et al (2010b) Design of arbitrarily homogeneous permanent magnet systems for NMR and MRI: theory and experimental developments of a simple portable magnet. J Magn Reson 205(1):75–85

Lindner J et al (2010) Efficiency optimization and prediction in high-gradient magnetic centrifugation. Chem Eng Technol 33(8):1315–1320

Lindner J, Menzel K,Nirschl H (2013a) Parameters influencing magnetically enhanced centrifugation for protein separation. Chem Eng Sci 97:385–393. doi:10.1016/j.ces.2013.04.044

Lindner J, Menzel K, Nirschl H (2013b) Simulation of magnetic suspensions for HGMS using CFD, FEM and DEM modeling. Comput Chem Eng 54:111–121. doi:10.1016/j.compchemeng.2013.03.012

Lindner J, Nirschl H (2014) A hybrid method for combining high-gradient magnetic separation and centrifugation for a continuous process. Sep Purif Technol 131:27–34

Langston PA, Tüzün U, Heyes DM (1995) Discrete element simulation of granular flow in 2D and 3D hoppers: dependence of discharge rate and wall stress on particle interactions. Chem Eng Sci 50(6):967–987

Svoboda J (2004) Magnetic techniques for the treatment of materials. Kluwer Academic Publishers, Dordrecht

Satoh A et al (1998) Stokesian dynamics simulations of ferromagnetic colloidal dispersions in a simple shear flow. J Colloid Interface Sci 203(2):233–248

Watson JHP (1973) Magnetic filtration. J Appl Phys 44(9):4209